Contribution of the Melting Stage to the Evolution of the Morphology and Chemical Conversion of Immiscible Polyamide/Polyethylene Blends in Twin-Screw Extruders

V. Yquel,[1,2] A. V. Machado,[1] J. A. Covas,[1] J. J. Flat[2]

[1]*Campus Azurem, University of Minho, 4800-058 Guimarães, Portugal*
[2]*Arkema, Cerdato, 27470 Serquigny, France*

Received 19 November 2008; accepted 5 April 2009
DOI 10.1002/app.30680
Published online 24 June 2009 in Wiley InterScience (www.interscience.wiley.com).

ABSTRACT: This study investigates the effects of processing conditions (the screw speed, throughput, barrel temperature, and screw configuration) on the chemical conversion and morphology evolution of polyamide/polyolefin blends along a twin-screw extruder. Polymer samples were collected rapidly at specific barrel locations with a special sampling device for subsequent chemical and morphological characterization. Increasing the screw speed or using more restrictive screw modules at the beginning of the melting zone promoted a faster reaction and better dispersion along the extruder. Increasing the throughput or decreasing the barrel temperature slowed the evolution of the morphology and chemical conversion along the extruder because of the lower melting rate. As soon as melting started, the chemical reaction took place. However, high chemical conversion rates required extensive melting, that is, significant interface generation. © 2009 Wiley Periodicals, Inc. J Appl Polym Sci 114: 1768–1776, 2009

Key words: blending; block copolymers; compatibilization; melt; reactive extrusion

INTRODUCTION

Polymer blending is an important route to the development of innovative materials. The performance of polymer blends depends essentially on the properties of their components and on their multiphase morphology. Reactive compatibilization is used extensively to control the size and stability of the dispersed phase and to improve the interfacial characteristics of immiscible polymer pairs.[1–4] During mixing, reactive functionalized polymers form *in situ* block or graft copolymers at the interface of the blend components. It is now clear that these graft or block copolymers induce a large reduction both in the interfacial tension and in the dispersed phase coalescence due to steric stabilization.[4,5]

For a given polymer pair, the blend composition, viscosity ratio, elasticity ratio, and interfacial tension determine the resulting morphology.[6–14] However, it has been shown that the morphology is also affected by the compounding conditions adopted (usually a corotating, self-wiping, intermeshing, twin-screw extruder is used), particularly the barrel temperature, residence time, screw speed, and screw profile,[6–14] that is, there is a practical need to define an adequate screw geometry and to select a feasible operating point if the required blend morphology is to be achieved. This issue is further complicated by the fact that, for a given operating condition, the evolution of the morphology (with time or, equivalently, along the screw length) is far from gradual, sudden changes in particle size or in chemical conversion having been reported. For example, Majumdar et al.[15] observed a progressive decrease in the particle size of the dispersed phase for a polyamide 6 (PA6)/styrene acrylonitrile physical blend, but for a compatibilized equivalent blend, they reported a dramatic reduction in the size of the dispersed droplets in the initial screw turns almost immediately after melting.

On the basis of the pioneering experiments performed in batch mixers with physical blends, Scott and Macosko[13] proposed a mechanism for initial morphology development involving the formation of sheets or ribbons of the minor component under the influence of local stresses, which become unstable and induce the creation of a two-dimensional network; when the latter also becomes unstable, particles or droplets are finally formed. This mechanism was reported as applicable to twin-screw extruders.[12,14,15]

In systems containing rubber and polyamide (PA)/polyesters, the rubber phase is dispersed from a millimeter level to a micrometer level within a few seconds.[16] This means a decrease in the diffusion

Correspondence to: A. V. Machado (avm@dep.uminho.pt).

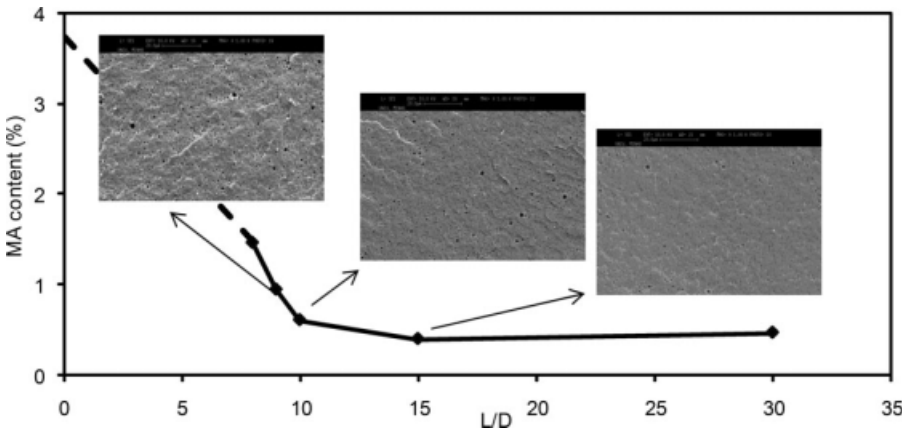

Figure 1 Morphology and chemical evolution along the extruder (80/20 w/w PA6/EPM-*g*-MA blend).

distance of the polycondensate chains toward the rubber interface by a factor of 10^3 and an increase in the interface by a factor of 10^9; that is, the rate of interfacial reactions is dramatically enhanced. In the case of PA6/maleic anhydride grafted ethylene propylene monomer (EPM-*g*-MA) blends, as new interfaces are generated upon melting, the fast reaction causes a sudden reduction of the interfacial tension preventing coalescence, which induces a further refinement of the dispersion.[17,18] To study this sequence experimentally, we developed an experimental methodology involving the quick collection of material from fully filled screw sections of the extruder.[19] Figure 1 shows a typical evolution of the chemical conversion [in terms of the percentage of the residual maleic anhydride (MA) content] and morphology along the screw axis, sampling points being located at length/diameter (L/D) values of 8, 9, 10, and 15 (the screw profile corresponds to configuration 1 in Fig. 2), as studied by Machado et al.[18] Although the material is mostly solid at $L/D = 8$, the unreacted MA content has decreased to less than half of its original value. One L/D value later, a fully melted conventional polymer blend morphology is present with relatively good distributive and dispersive mixing levels, a further important reduction in MA having been caused. Thus, although the sampling methodology has been used successfully to monitor the evolution of the rheology, morphology, and chemical conversion of various polymers or composite systems,[18,20,21] in some cases, it is unable to provide an unambiguous and detailed description of the compatibilization and morphology development mechanisms.

This work was aimed at monitoring in greater detail such phenomena in a fast reacting polymer blend system with two approaches: (1) developing a sampling methodology able to provide material samples at each 0.5 L/D value along the screw axis and (2) performing experiments under a variety of processing conditions, some of them favoring and others retarding the evolutions to be studied.

EXPERIMENTAL

Materials

Commercial injection-type, low-viscosity PA6 and polyethylene (PE) were used as blend components, whereas PE bearing MA species was used as a compatibilizer. The composition of the blends was such that a PA6 matrix with polyolefin (PO) nodules was always ensured.

Preparation of the blends

The blends were prepared in a Leistritz (Nuremberg, Germany) LSM 30.34 laboratory, modular, intermeshing, corotating, twin-screw extruder and subsequently pelletized with the appropriate downstream equipment (a water-through, blown-air drier and a rotary cutter). Table I shows the processing conditions used in each experiment, which corresponded to the different settings of the throughput (which varied between 5 and 15 kg/h), screw speed (which varied between 50 and 300 rpm), barrel temperature (either a constant value of 260°C or an increasing profile in the downstream direction), or screw profile. Figure 2 illustrates the general extruder layout and identifies the two screw configurations, which differ in terms of the staggering angle of the kneading block

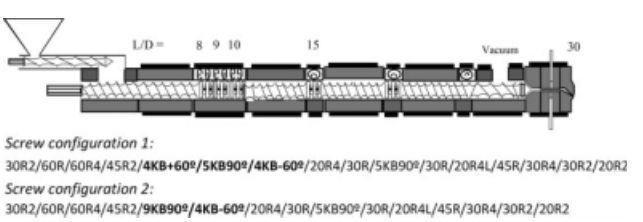

Figure 2 Extruder layout and screw configurations.

TABLE I
Processing Conditions

Throughput (kg/h)	Screw speed (rpm)	Screw configuration	Temperature (°C)
15	100	1	260
15	200	1	260
15	300	1	260
5	50	1	260
5	100	1	260
5	300	1	260
5	50	2	260
5	100	2	260
5	200	2	260
5	300	2	260
15	300	2	260
15	300	1	180–200–260
15	300	2	180–200–260

upstream, configuration 1 having been adopted in previous research.[21] Although both kneading blocks comprise 13 kneading disks, configuration 1 contains 4 disks staggered +60°, five staggered 90°, and 4 staggered −60°, whereas configuration 2 contains 9 disks staggered 90° and four staggered −60°. In other words, configuration 2 is more restrictive than configuration 1.

Figure 2 shows also the location of the sampling devices. These consist basically of rotating valves that create material flow from inside the extruder via a lateral hole in the barrel and expose it for manual removal (a more complete description of this tool is available[12]). The operation takes 1–2 s, and the sample is immediately quenched in liquid nitrogen to avoid further morphological or chemical evolution. Because sample collection is facilitated by pressure flow, these devices are generally positioned adjacent to screw sections that work fully filled, typically kneading blocks, or left-handed elements, in which most of the physicochemical phenomena are expected to occur.

For the purposes of this work, the original Leistritz extruder barrel segment (ca. 120 mm long) enveloping the first kneading block upstream was replaced by a home-made segment of equal length containing identical heating and cooling features for temperature control as well as 6 sampling devices equally distributed every 15 mm along its axis. Because each extruder screw diameter was 30 mm, this meant that samples could be collected at each 0.5 L/D value upon the melting of the blend components.

Material characterization

The overall experimental procedure is summarized in Figure 3.

Samples obtained from *in situ* compatibilization were milled and dried overnight, and this was followed by hydrolyzation with hydrochloric acid for 6 h and subsequent filtering, washing with water, and drying for 1 h at 180°C to convert dicarboxylic acid back into anhydride.[13] Thin films were prepared by compression molding and characterized by Fourier transform infrared (model 1600 spectrometer, PerkinElmer). The anhydride carbonyl peak at 1785 cm^{-1}, together with an IR calibration rule determined with a set of references, allowed the quantitative determination of the residual MA content.[17] Chemical conversion was defined as the difference between the initial and residual amounts of MA divided by the initial value.

After etching of the samples with boiling xylene (refluxing for 1 h) to remove the PO from the surface and gold plating (1 nm), the morphology of the blends was studied by scanning electron microscopy (SEM) with a JEOL JSM 6310F scanning electron microscope.

The average particle size and the particle size distribution of the dispersed phase were determined with an automatic method of image analysis (Quantimet 550, Leica), with an equivalent diameter assumed for each particle. To obtain representative results, at least 100 particles were studied in each picture.

RESULTS AND DISCUSSION

Effect of the screw speed

Figure 4 combines SEM micrographs of samples obtained along the screw axis (in the first and

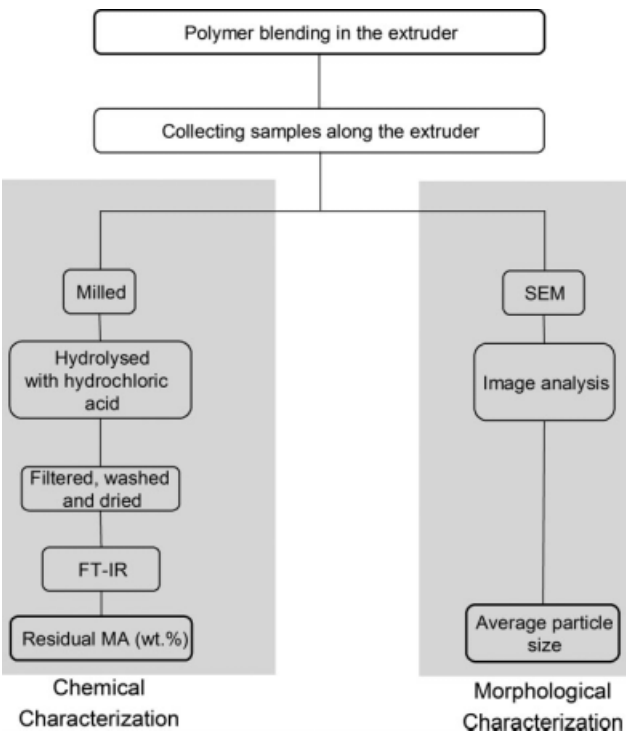

Figure 3 Experimental procedure for material characterization.

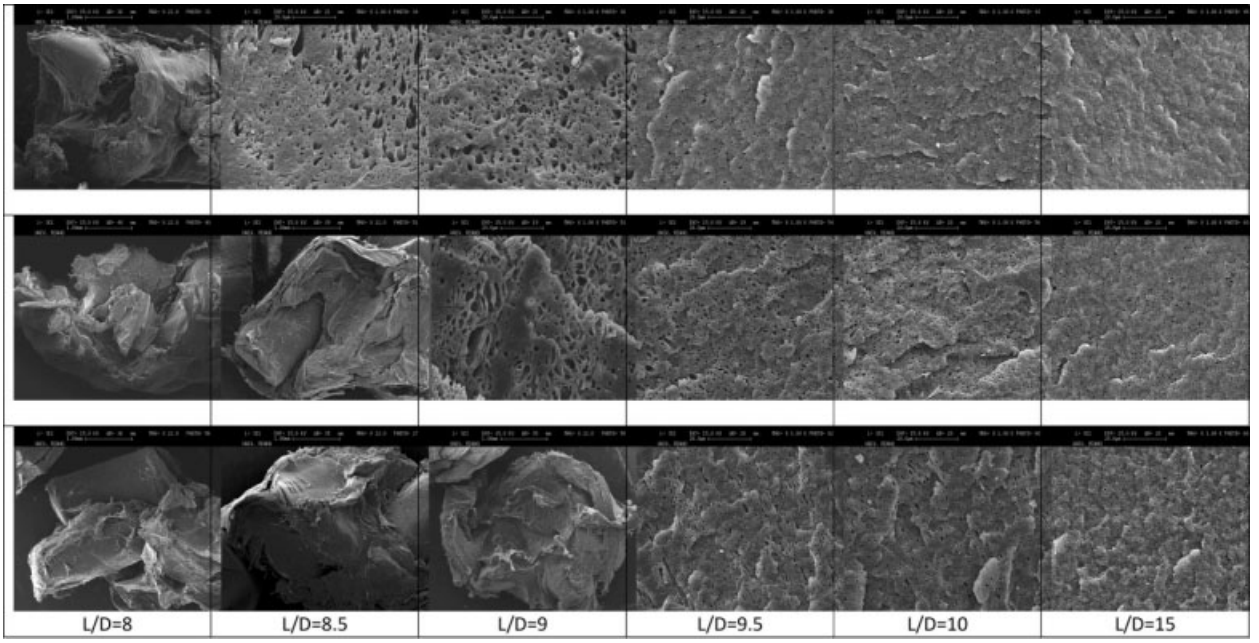

Figure 4 Blend morphology along the extruder for different screw speeds (screw configuration 1 with a throughput of 15 kg/h and with the barrel temperature set at 260°C): 300 (top row), 200 (middle row), and 100 rpm (bottom row).

second kneading blocks; see Fig. 2) for various screw speeds (screw configuration 1 with a throughput of 15 kg/h). It is interesting to observe the high efficiency of melting in the corotating, twin-screw extruders, which is in agreement with previous reports.[20,21] In fact, in the three cases, within 0.5 L/D, there is a quick transition from an essentially unmelted material to a more or less homogeneous melt. Anyway, although at 300 rpm a stable morphology seems to be achieved around $L/D = 9.5$, at 100 rpm, this happens only at $L/D = 15$. The underlying reason for this behavior is also shown in Figure 4: increasing screw speeds foster melting and, for this reason, interface generation due to the complex flow pattern that takes place in the kneading blocks. In principle, at a constant throughput, an increase in the screw speed would lower the number of fully filled channels upstream of any restrictive elements. For the kneading block upstream, as in this case, this worsens the conditions for heat transfer and melting onset. However, as shown in Figure 4 for this particular polymer blend, at high screw speeds, the eventual delay in the initiation of melting is more than compensated by the higher thermomechanical stresses (and contribution to heating from viscous dissipation); that is, melting becomes more efficient. Figure 5(a) presents the corresponding evolution of the average particle size. The effect of the screw speed at a low throughput (5 kg/h) has also been included. All curves contain the same three features in the downstream direction: a high initial slope corresponding to a change in scale from millimeters to submicrometers in a very short axial distance (dotted lines), a steady (ca. 2-fold) decrease down to 0.3–0.4 μm, and a plateau (until the die outlet). The first characteristic obviously corresponds to melting of the solid pellets. In fact, in the series of

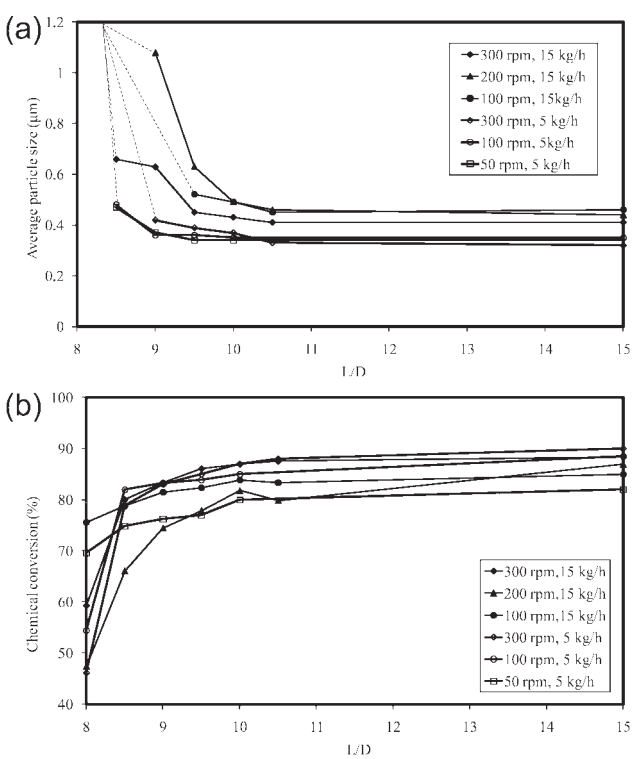

Figure 5 Evolution of (a) the dispersed particle size and (b) the chemical conversion along the extruder for different screw speeds and throughputs (screw configuration 1 with the barrel temperature set at 260°C).

micrographs of Figure 4 for 100 and 200 rpm, it is possible to identify at $L/D = 8.5$ solid pellets of PA6 surrounded by molten PO. In the intermediate stage, the dispersed phase decreases in size, and its particles becoming progressively less elongated and more regular (see the same micrograph series in Fig. 4). The plateau evidences little change.

Thus, despite the differences upstream between the curves, from $L/D = 10.5$ onward, the average particle size becomes relatively constant. In fact, in all cases, no differences in morphology were noticed beyond $L/D = 15$; hence, no data are presented. The higher the screw speed is, the faster the morphology becomes constant. It is difficult to establish a correlation between the average particle size and screw speed, although there seems to be a tendency for higher screw speeds leading to finer dispersions. Figure 6(a) contributes with more data on this topic by comparing the evolution in the particle size along the screw axis for different screw speeds when screw configuration 2 is used. As the screw speed is increased, the initial particle size at the section of the curve corresponding to a sudden particle size reduction decreases, and the average size of the dispersed phase decreases, the morphology being well developed at $L/D = 10$.

The chemical conversion is shown in Figures 5(b) and 6(b) for the same morphology data reported in Figures 5(a) and 6(a), respectively. Again, three features are worthy of discussion. First, at $L/D = 8$ (beginning of the kneading block), where, as discussed previously, an essentially solid sample was collected, the degree of conversion ranges between 45 and 80%. In the case of configuration 2, which is more restrictive than configuration 1, 77–82% chemical conversions have already been attained at $L/D = 8$. At the end of the same kneading block ($L/D = 10$), conversions reach 80–88% (the final conversions, at the die outlet, are within the same range). As discussed in previous studies,[17,18] this emphasizes again the fact that the chemical reaction between amine and anhydride groups is very rapid, requiring only partial melting of one of the components, as this provides sufficient temperature and interface generation. In all cases, the degree of conversion for the lowest screw speed at $L/D = 8$ is higher than that for the rest. This should be related to the fact that, as previously discussed, at lower speeds the screws become fully filled more upstream, and this promotes earlier melting onset, but the melting rate is lower (i.e., a longer axial length for melting).

Second, between $L/D = 8$ and $L/D = 10.5$, chemical conversion increases rapidly, but with a progressively slower pace. The rate of increase in chemical conversion at 50 or 100 rpm is much lower than that at 200 or 300 rpm. Although the behavior is similar for 200 or 300 rpm, the final rate of conversion is higher for 300 rpm because of the higher value at $L/D = 8$.

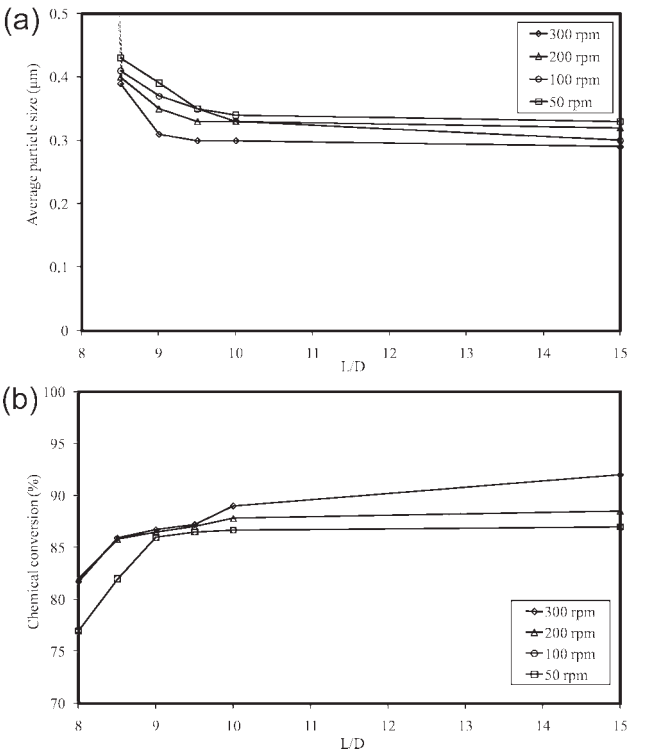

Figure 6 Evolution of (a) the dispersed particle size and (b) the chemical conversion along the extruder for different screw speeds (screw configuration 2 with a throughput of 15 kg/h and with the barrel temperature set at 260°C).

Third, beyond $L/D = 10.5$, the chemical conversion does not change.

These results indicate that higher screw speeds may delay the onset of melting in the extruder because they cause a decrease in the number of fully filled screw channels. However, once melting is initiated, a high rpm value guarantees an efficient melting rate by creating high shear stresses and a complex flow field. Since the beginning of melting, interfaces are generated between the two polymers, inducing high chemical conversion rates. A chemical reaction takes place as soon as melting begins, in the early stages of morphology development. The reaction continues progressively during melting until a fully developed morphology is achieved. As soon as the copolymer is formed at the interface, it stabilizes the dispersed phase, hindering phenomena such as coalescence. Even though chemical conversion is lower than 100% at $L/D = 10.5$, it does not change downstream. This has been observed before[17,18] and attributed to the fact that the residual MA groups are probably located inside the PO particles and not at the interface, consequently opposing further conversion. A decrease in the MA content was measured when one of the polymers began to melt, and this is in line with previous reports.[17,18] Therefore,

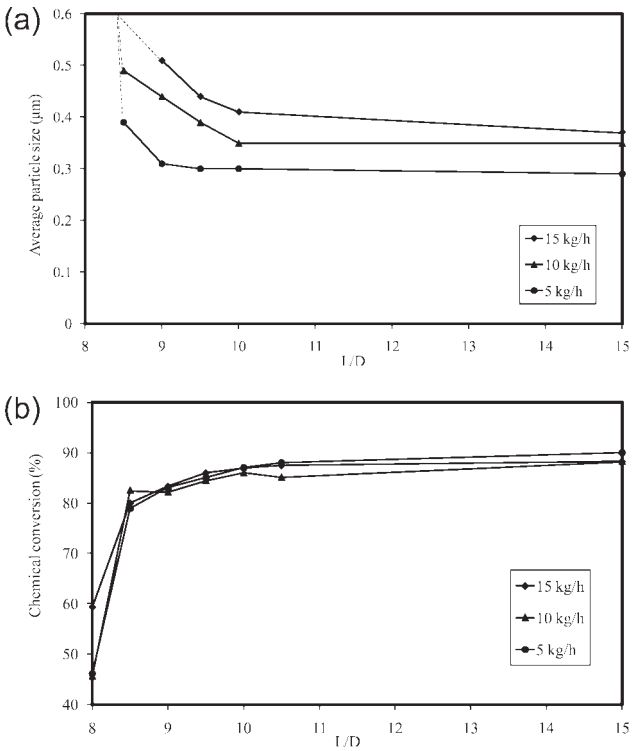

Figure 7 Evolution of (a) the dispersed particle size and (b) the chemical conversion along the extruder for different throughputs (screw configuration 2 at 100 rpm with the barrel temperature set at 260°C).

for this polymer system, which includes a very fast reaction, chemistry takes place before morphology development.

Effect of the throughput

The effect of the throughput on morphology development in terms of the particle size can be inferred by the observation of Figures 5(a) and 7(a) for screw configurations 1 and 2, respectively. SEM micrographs of the samples removed along the screw can be visualized in Figure 8 for screw configuration 2. The differences are quite clear. Higher throughputs delay morphology development and may yield coarser particle sizes, most likely because the residence time for mixing and reacting during flow in the kneading blocks is shorter.

Figures 5(b) and 7(b) show the chemical conversion evolution for the data pictured in Figures 5(a) and 7(a), respectively. Interestingly, at the beginning of the kneading block, the chemical conversion for higher throughputs is higher than that for lower throughputs, but the rates of chemical conversion in the downstream direction are different. Most likely, unlike the effect of the screw speed, the variation in the initial value is due to the fact that higher throughputs will promote earlier filling of the screw channels with more efficient heat transfer; hence, chemical conversion is initiated, even if solids are present in a high percentage. However, as residence times are also short, melting is slower, and this explains the lower conversion rates downstream.

Effect of the temperature profile

As indicated in Table I, most of the experiments were performed with a set flat barrel–die profile of 260°C, but a profile increasing from 180°C at the material inlet to 260°C at the third barrel segment (just upstream of the second mixing zone, see Fig. 2) was also used (this profile is denoted as 180–200–260°C), as it was anticipated that it could slow down the evolution of morphology and chemical conversion along the kneading block.

The effect of temperature on morphology development is shown in Figure 9, all other processing conditions being kept constant (at $L/D = 8$, the sample consisted of loose pellets). It is clear from the SEM micrographs that morphology development is delayed when the temperature profile is used. Nevertheless, melting is still quick because at $L/D =$

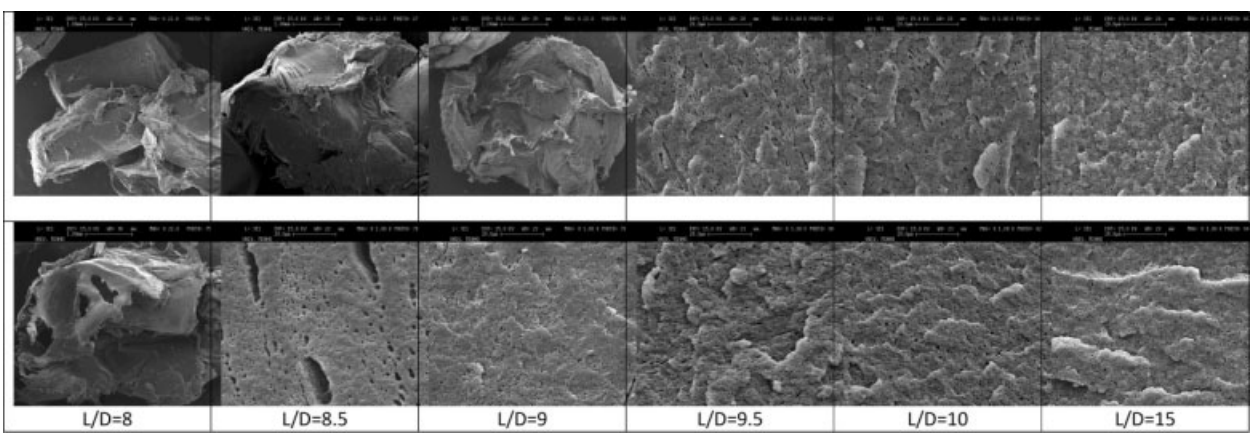

Figure 8 Morphology of the blend along the extruder for two different throughputs (screw configuration 2 at 100 rpm with the barrel temperature set at 260°C): 15 (top row) and 5 kg/h (bottom row).

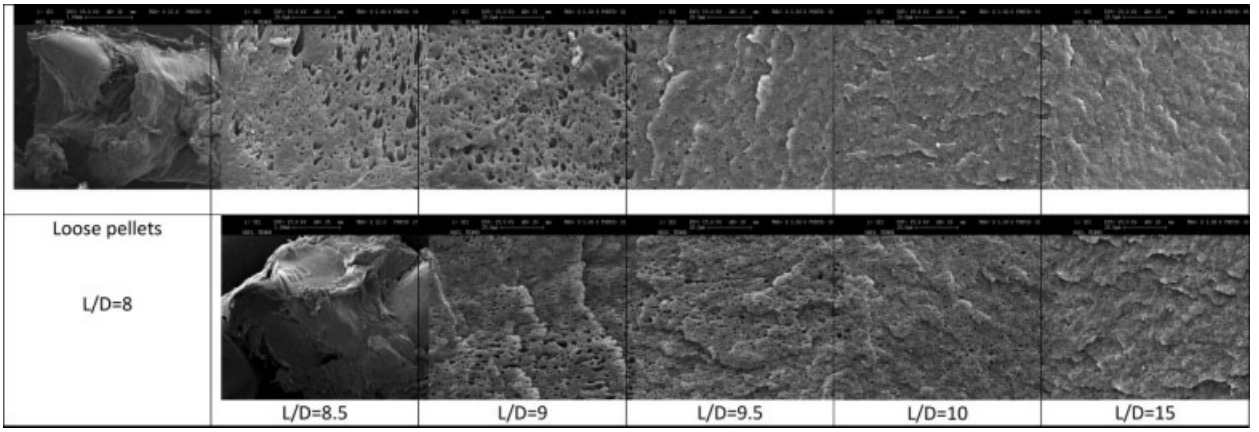

Figure 9 Morphology of the blend along the extruder with a flat set temperature profile (top row) and with an increasing set temperature profile (bottom row; screw configuration 1 at 300 rpm and 15 kg/h).

8.5, it is possible to detect both melted and solid particles; at $L/D = 9$, melting is complete, and the morphology consists of a dispersed phase with large, elongated particles; at $L/D = 9.5$, the dispersed particle size is smaller; and well-dispersed particles are visible at $L/D = 10$. As discussed previously, when a constant temperature profile is used, a fully developed morphology is obtained at $L/D = 9.5$. Figure 10(a) shows a parallel evolution of the average particle size along the extruder; hence, the final particle size of the dispersed phase is lower when a constant temperature profile is used.

With the exception of a single experimental point, the evolution of chemical conversion [Fig. 10(b)] is also parallel, the final value being lower for the nonuniform temperature profile.

Thus, the results demonstrate that temperature plays a major role in both chemical conversion and morphology development. Lower set temperatures at the beginning of the first kneading block delay the achievement of a stable morphology and prevent high chemical conversions from being reached.

Effect of the screw configuration

As explained previously, the 4 kneading disks upstream staggered at +60° in screw configuration 1 are replaced by 4 discs staggered at 90° in screw configuration 2 (see description in Fig. 2). Accordingly, configuration 2 is more restrictive than configuration 1; that is, it should create flow and thermal conditions promoting faster chemical conversion and morphology evolution because not only more screw channels are fully filled upstream but also more mixing and viscous dissipation are promoted during flow along the kneading block.

Even though the rate of morphology development (Fig. 11) seems similar for both configurations, a smaller dispersed particle size is obtained with screw configuration 2, as shown in Figure 12(a), which illustrates the differences in the evolution of the average particle size for the two screw configurations for different screw speeds (with a constant throughput of 5 kg/h and the barrel temperature set at 260°C). The higher the screw speed is, the more noticeable the differences are in the rate of size reduction and in the final average size of the dispersed phase, configuration 2 being the most efficient.

When the effect of the screw speed or throughput on chemical conversion was being studied, it was

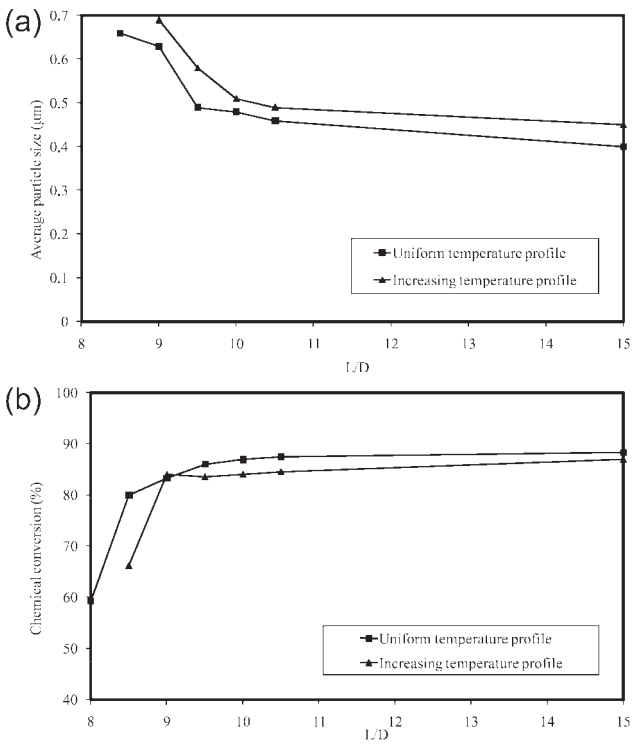

Figure 10 Evolution of (a) the dispersed particle size and (b) the chemical conversion along the extruder with a flat set temperature profile and an increasing set temperature profile (screw configuration 1 at 300 rpm and 15 kg/h).

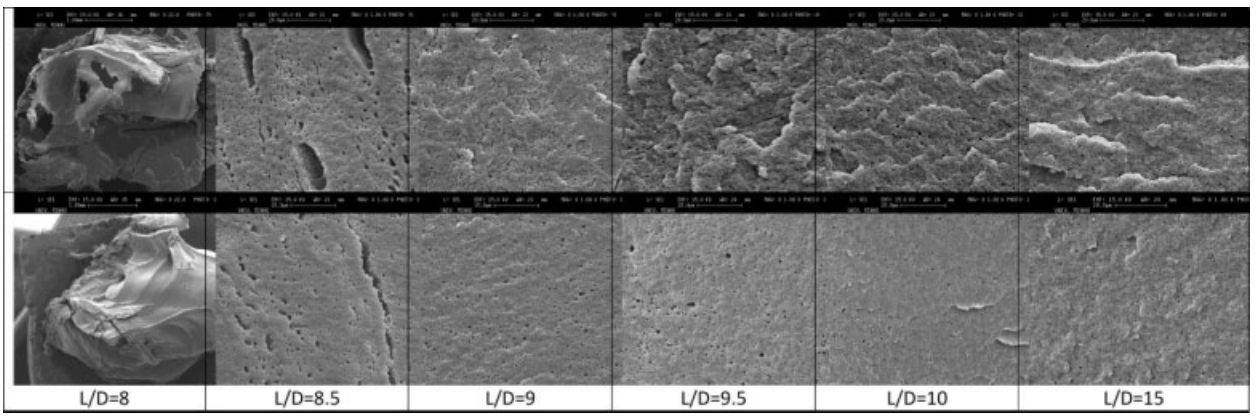

Figure 11 Morphology of the blend along the extruder for two different screw configurations (at 5 kg/h with the barrel temperature set at 260°C): screw configuration 1 (top row) and screw configuration 2 (bottom row).

argued that higher initial values of chemical conversion at $L/D = 8$ did not necessarily mean a more efficient morphology/chemical evolution along the kneading block, as they simply mirrored the longer material residence times at fully filled channels upstream of the kneading block. However, as shown in Figure 12(b), the use of restrictive blocks favors chemical conversion both upstream, because of the formation of more fully filled channels in which heat transfer is more efficient, and along its length, because of a more complex, more intensive, and lengthier flow along its length.

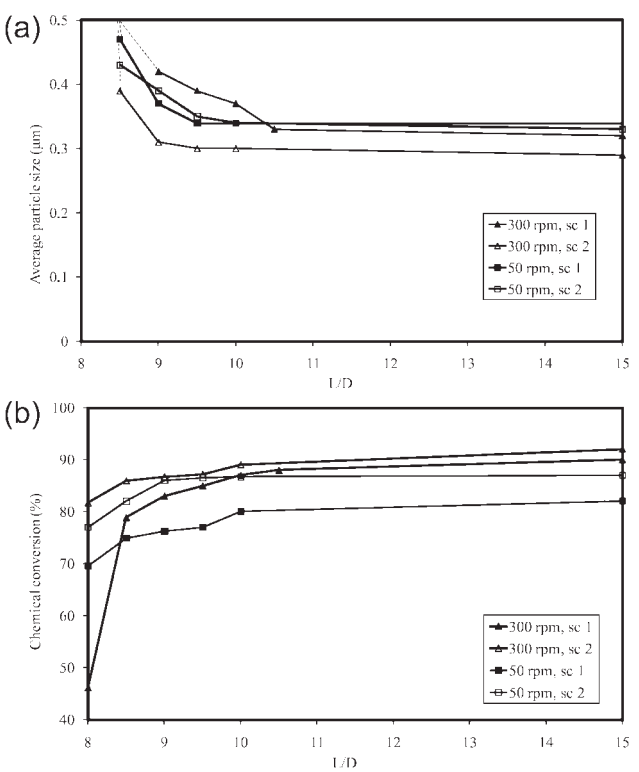

Figure 12 Evolution of (a) the dispersed particle size and (b) the chemical conversion along the extruder for two different screw configurations and screw speeds (at 5 kg/h with the barrel temperature set at 260°C).

Overview on the contribution of melting

The data presented and discussed throughout this work seem to indicate that melting (onset location and rate) is the decisive parameter affecting chemical conversion and morphology evolution of a fast reactive compatibilization system. In turn, melting features are controlled by screw design as well as operational parameters. As soon as one of the polymer pair components melts, it surrounds, even if partially, the surface of the pellets of the other polymer. The interface thus generated allows high conversion ratios to be quickly attained. However, this step has little effect on morphological development. The solid polymer pellet may be progressively

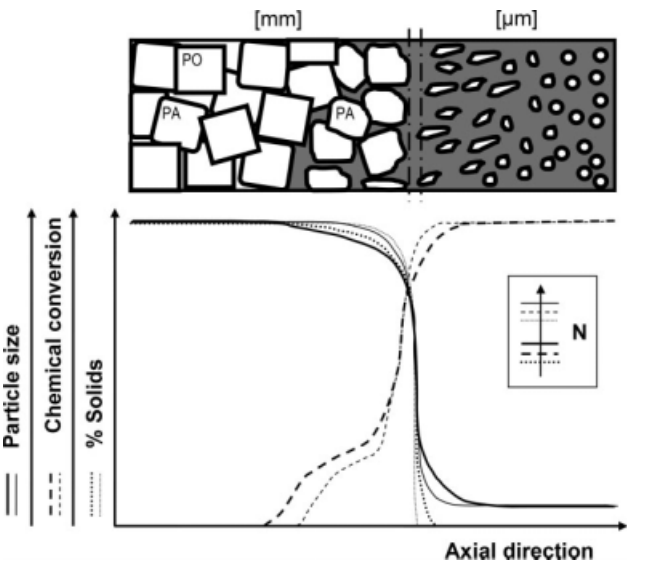

Figure 13 Schematic evolution of the physicochemical processes along the extruder during reactive polymer blending.

distorted because of the combined action of heat and shear, but no major gains in chemical conversion can be obtained at this stage, as these deformations do not generate new orders of magnitude of interfacial area. Hence, for some processing conditions, slow melting can hold back chemical conversion. Considerable gains in interfacial area require full melting of the surviving solids. As their melting occurs and a dispersed phase is created, formation of the copolymer (i.e., a further increase in chemical conversion) helps to stabilize quickly the size and shape of the suspended particles, which evolve quickly from large, elongated particles to submicrometer regular units. This sequence of events is schematized in Figure 13, which illustrates also the effect of the screw speed.

Higher screw speeds delay the onset of melting in the extruder because they cause a decrease in the number of fully filled screw channels (lower residence time, less efficient heat transfer), and so at the beginning of the first kneading block, the average degree of conversion is lower in comparison with that for lower speeds. However, once the process is initiated, higher screw speeds promote more efficient melting because of higher shear rates and friction; hence, new polymer–polymer interfaces are created at a greater pace, and chemical conversion increases more pronouncedly.

CONCLUSIONS

This study was focused on the effects of processing conditions (the screw speed, throughput, barrel temperature, and screw configuration) on the chemical conversion and morphology evolution of PA/PO blends along a twin-screw extruder. To achieve this, polymer samples were collected rapidly at specific barrel locations with a special sampling device, and this was followed by chemical and morphological characterization.

Increasing the screw speed or using more restrictive screw modules at the beginning of the melting zone promotes faster reactions and better dispersion along the extruder, and this means that both have a strong effect on the distributive and dispersive mixing rates and intensity. Conversely, increasing the throughput slows the evolution of the blend morphology along the extruder. For obvious reasons, decreasing the barrel temperature delays the blend compatibilization because of slower melting.

Some of the operating conditions allow the morphology development and the chemical conversion in the first kneading zone to be slowed and a better perception of the interrelationship between the chemistry and morphology to be obtained. As soon as melting is promoted by the presence of fully filled screw channels, the chemical reaction takes place and reaches important levels. However, high chemical conversion rates require extensive melting, that is, substantial interface generation. Under these conditions, quick morphology development occurs and becomes stable because of the simultaneous copolymer formation.

In view of the experiments performed and of the experimental data generated, it has been demonstrated that the melting stage (in terms of both the location of its onset and its development rate) greatly influences the chemical conversion and morphology evolution of a fast reactive compatibilization system.

References

1. Kim, M. J.; Yoo, J. E.; Choi, H. K.; Kim, C. K. Macromol Res 2002, 10, 91.
2. Gong, L.; Friend, A. D.; Wool, R. P. Macromolecules 1998, 31, 3706.
3. Boucher, E.; Folkers, J. P.; Creton, C.; Hervert, H.; Leger, L. Macromolecules 1997, 30, 2102.
4. Cho, K.; Li, F. Macromolecules 1991, 24, 2752.
5. Creton, C.; Hooker, J.; Shull, K. R. Langmuir 2001, 17, 4948.
6. Miles, I. S.; Zurek, A. Polym Eng Sci 1988, 28, 796.
7. Ho, R. M.; Wu, C. H.; Su, A. C. Polym Eng Sci 1990, 30, 511.
8. Favis, B. D.; Therrien, D. Polymer 1991, 32, 1474.
9. He, J.; Bu, W.; Zeng, J. Polymer 1997, 38, 6347.
10. Shih, C.-K. Polym Eng Sci 1995, 35, 1688.
11. Sundararaj, U.; Macosko, C. W.; Shih, C.-K. Polym Eng Sci 1996, 36, 1769.
12. Sundararaj, U.; Macosko, C. W.; Rolando, R. J.; Chan, H. T. Polym Eng Sci 1992, 32, 1814.
13. Scott, C. E.; Macosko, C. W. Polymer 1995, 36, 461.
14. Lee, J. K.; Han, C. D. Polymer 2000, 41, 1799.
15. Majumdar, B.; Paul, D. R.; Oshinski, A. J. Polymer 1997, 38, 1787.
16. Duin, M.; Gurp, M.; Leemans, L.; Walet, M.; Aussems, M.; Martin, P.; Legras, R.; Machado, A. V.; Covas, J. Macromol Symp 2003, 198, 135.
17. Machado, A. V.; Covas, J. A.; Duin, M. J Polym Sci Part A: Polym Chem 1999, 37, 1311.
18. Machado, A. V.; Covas, J. A.; Duin, M. J Appl Polym Sci 2001, 80, 1535.
19. Machado, A. V.; Covas, J. A.; Duin, M. J Appl Polym Sci 1999, 71, 136.
20. Covas, J. A.; Carneiro, O. S.; Maia, J. M.; Filipe, S. A.; Machado, A. V. Can J Chem Eng 2002, 80, 1065.
21. Machado, A. V.; Yquel, V.; Covas, J. C.; Flat, J.-J.; Ghamri, N.; Wollny, A. J. Macromol Symp 2006, 233, 86.